Ultrasound Obstet Gynecol 2010; **35**: 302–309
Published online 22 December 2009 in Wiley InterScience (www.interscience.wiley.com). **DOI:** 10.1002/uog.7530

Fetal interrupted aortic arch: 2D-4D echocardiography, associations and outcome

P. VOLPE*, G. TUO†, V. DE ROBERTIS*, G. CAMPOBASSO*, M. MARASINI†, A. TEMPESTA*, M. GENTILE‡ and G. REMBOUSKOS*

**Fetal Medicine Unit, Di Venere and Sarcone Hospitals and ‡Department of Medical Genetics, Hospital Di Venere, ASL Bari and †Pediatric Cardiology IRCSS G. Gaslini, Genoa, Italy*

KEYWORDS: 22q11.2 microdeletion; B-flow; congenital heart disease; CORSA; fetal echocardiography; interrupted aortic arch; prenatal diagnosis; STIC; three/four-dimensional ultrasound

ABSTRACT

Objectives *To analyze fetal two-dimensional (2D) echocardiographic characteristics of interrupted aortic arch (IAA) and its different types, to explore whether the use of 4D ultrasound with B-flow imaging and spatiotemporal image correlation (STIC) can improve prenatal diagnostic accuracy, and to describe associations and outcome.*

Methods *The study comprised IAA fetuses examined exclusively by 2D conventional echocardiography during the period from 1994 to 2003, and those identified by conventional echocardiography and examined further by 4D ultrasound with B-flow imaging and STIC during the period January 2004 to July 2008, identified among fetuses examined at two referral centers for congenital heart defects (CHD). Postnatal follow-up was available in all cases. Karyotyping and fluorescent in-situ hybridization (FISH) analysis for the DiGeorge critical region (22q11.2) were performed in all cases.*

Results *Twenty-two cases of isolated IAA (15 Type B and seven Type A, seven and three of which, respectively, underwent B-flow imaging and STIC) were detected among 2520 cases of fetal CHD. In seven of the 15 Type B cases, a right subclavian artery arose anomalously (ARSA). 2D echocardiography failed to distinguish the type of IAA in only two cases and the ARSA in five of the seven cases. B-flow imaging and STIC successfully identified IAA types in all 10 cases examined and clearly visualized the origin and course of the ARSA, including cervical ones. FISH detected 22q11.2 microdeletion in 10 of the 15 Type B cases and an unusual association with Type A in one of the seven cases. Fetal/neonatal outcome included: eight terminations of pregnancy, one intrauterine death and four postoperative deaths in the neonatal period, and nine neonates were alive after surgery at a mean follow-up time of 58 months (range, 4 months–13 years).*

Conclusion *Our results confirm the feasibility of prenatal characterization of IAA and its different types based on 2D echocardiographic examination, albeit with some limitations in the thorough assessment. 4D ultrasound with B-flow imaging and STIC can apparently facilitate visualization and detailed examination of the anatomical features of the IAA types, including visualization of the neck vessels, thus supplying additional information with respect to 2D sonography. As for the known association with microdeletion 22q11.2, our data indicate that Types A and B are distinct, there being a close association only with IAA Type B.*

INTRODUCTION

Interruption of the aortic arch (IAA) is a rare, severe form of congenital heart defect (CHD) characterized by complete anatomical discontinuity between two adjacent segments of the aortic arch. Three anatomical types have been described according to the site of interruption: in Type A the interruption is distal to the left subclavian artery; in Type B it is between the left carotid and left subclavian arteries; and in Type C it is between the innominate artery and the left carotid artery[1,2]. In postnatal studies, IAA Type A is rarely associated with 22q11.2 deletion[3], whereas Type B is associated with this and other extracardiac features in 50–80% of cases[4–6], often in the context of specific syndromes. Type C is by

Correspondence to: Dr P. Volpe, Fetal Medicine Unit, Hospital Di Venere, ASL Bari, via Ospedale Di Venere, 70100 Bari, Italy (e-mail: paolo-volpe@libero.it)

Accepted: 19 August 2009

far the least common form of IAA, accounting for fewer than 5% of cases. Prenatal diagnosis of IAA has been reported in few case series[7,8].

Recently, four-dimensional (4D) ultrasound has been suggested to provide a significant contribution to our understanding of the developing heart in both normal and anomalous cases[9–15]. In particular, B-flow imaging and spatiotemporal image correlation (STIC) have been shown to supply additional information over that provided by two-dimensional (2D) ultrasound in the prenatal diagnosis of some cardiac defects[15–17] due to the ability to trace the spatial course of the vessels involved in the anomaly and to facilitate the identification of small vessels (Figure 1).

We report herein a fetal case series of isolated IAA, in an attempt to evaluate the reliability of 2D echocardiography in the prenatal characterization of this anomaly and its types, and to explore whether the use of 4D ultrasound with B-flow imaging and STIC can improve prenatal diagnostic accuracy. In addition, we describe associations and outcome of IAA when diagnosed in the fetus in a multicenter series of 22 cases.

METHODS

This study was performed at two referral centers for CHD (Fetal Medicine Unit, Di Venere and Sarcone Hospitals, ASL Bari and Pediatric Cardiology IRCSS G. Gaslini, Genoa). We first conducted a retrospective study covering the 10-year period from 1994 to 2003 to identify all cases in which IAA was diagnosed *in utero*. In all cases 2D fetal echocardiography had been performed with an ultrasound system equipped with pulsed, continuous and color Doppler capability (Prosound 5000, Aloka, Tokyo, Japan; Hewlett Packard Sonos 550, Andover, MA, USA). Thereafter, we evaluated whether the use of 4D ultrasound with STIC would improve the prenatal assessment of IAA and its types. To this end, from January 2004 until July 2008, all cases diagnosed with IAA on 2D echocardiography at the centers were further examined using 4D ultrasound with B-flow imaging and STIC (Voluson 730 Expert and Voluson E8, GE Medical Systems, Zipf, Austria). Fetuses with associated major heart defects were excluded from analysis and one case was excluded from the second part of the study because a postmortem examination was not performed. In all cases included in the study, the diagnosis of IAA was established conclusively by postnatal computed tomography, surgery and/or autopsy.

The clinical files of all IAA cases diagnosed and managed at the two institutions in the first study period (1994–2003) were retrieved from a computerized database. The following variables were available for analysis in all cases: indication for fetal echocardiography, associated extracardiac and chromosomal anomalies and fetoneonatal outcome. The following quantitative echocardiographic parameters were also analyzed: atrial and ventricular dimensions, aorta and pulmonary artery diameters, and ratios between right and left heart structures. These measurements were compared with established normal values[18]. In addition, we analyzed the course of the ascending aorta (AAo) and neck vessels by color Doppler.

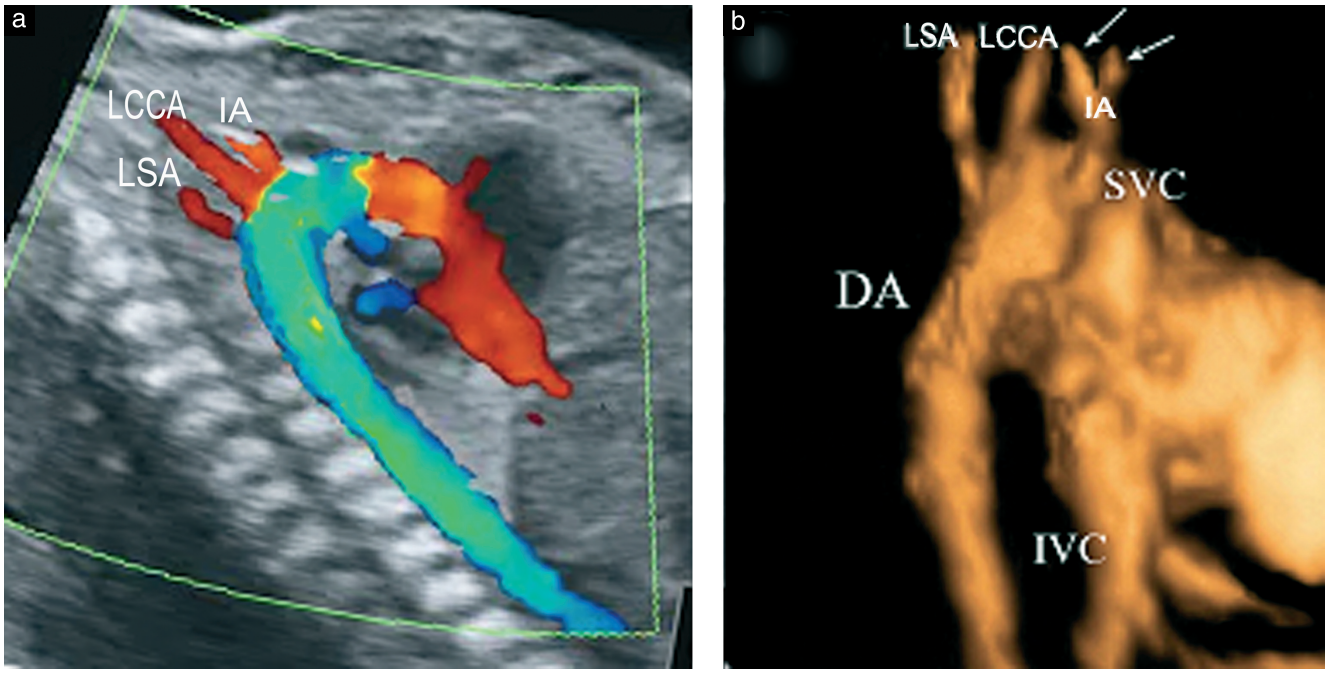

Figure 1 (a) Two-dimensional color Doppler image at 23 weeks of a normal fetal aortic arch, showing the origins of the three neck vessels (innominate artery (IA), left common carotid artery (LCCA) and left subclavian artery (LSA)). (b) B-flow and spatiotemporal image correlation showing the three neck arteries. The right common carotid artery and the right subclavian artery (arrows) are also clearly visible. DA, descending aorta; IVC, inferior vena cava; SVC, superior vena cava.

In the second part of the study, after 2D and color Doppler evaluation of each case, the sagittal view of the heart was visualized and heart volume datasets were acquired with B-flow imaging and STIC using automatic sweeps through the fetal thorax. The volume of interest was acquired with a sweep angle of approximately 20–35° (depending on the size of the fetus), sufficient to include the stomach, the heart with its vascular connections and the neck vessels. The acquisition time lasted between 7.5 and 12.5 s. B-flow settings during acquisition were: sensitivity, 4 and persistence, 2. Volume datasets were displayed initially using multiplanar slicing and the original plane of acquisition was displayed in Panel A (upper left panel) of the screen. Then volume rendering was applied to the dataset and the 3D image with the same orientation as that in Panel A was displayed in the lower right panel of the screen. The region of interest was adjusted in an attempt to display a thick-slice rendering comprising the fetal heart and its vascular connections, the AAo, the neck vessels and the whole aortothoracic tract. Surface rendering was performed with a mixture of gradient light plus surface algorithms. Postprocessing adjustments were performed to improve the image quality: the transparency level was set to 20, and the threshold level at 70–80. Rotation of the 3D image along the *x*-, *z*- and *y*-axes was performed until the structures of interest were visualized. The rendered images were analyzed to assess the course and size of the AAo, and to evaluate the anatomy and route of the neck vessels. To obtain optimal images, the 4D images were frozen and the most informative volume dataset within the cardiac cycle was chosen.

Karyotyping and fluorescent *in-situ* hybridization (FISH) for the DiGeorge critical region (22q11.2) were performed in all cases. In six cases (Cases 2, 6, 12, 16, 21 and 22), the fetal karyotype had been analyzed previously by amniocentesis/villocentesis due to maternal age or positive nuchal translucency screening. In the remaining cases, karyotyping was performed after detection of IAA, either prenatally or, in four cases (Cases 8, 14, 15 and 18), postnatally, according to the gestational age at the time of detection and the parents' expectations. If the chromosome 22 microdeletion was detected, permission to perform FISH analysis in the parents themselves was requested in order to determine the inheritance pattern. In all cases, slides were processed for FISH using the following probes: N25 (D22S75 within 22q11.2)/WI-941 (within 22q13) supplied by ONCOR (Gaithersburg, MD, USA) and TUPLE 1 (within22q11.2)/ARSA (arysulfatase A within 22q13.31 – qter) supplied by Vysis (Downers Grove, IL, USA).

RESULTS

Prevalence of isolated interrupted aortic arch and association with 22q11 microdeletion

Over the 14-year period, among 2520 cases of CHD we identified 22 (0.87%) fetuses with isolated IAA (in the absence of major heart defects): 15 Type B and seven Type A. Of these, 12 (eight Type B and four Type A) were detected in the period from 1994 to 2003 and 10 (seven Type B and three Type A) between January 2004 and July 2008. The mean gestational age at diagnosis was 24 (range, 20–35) weeks, with 12 cases being diagnosed before 24 weeks' gestation. The indication for fetal echocardiography and the type of IAA in each case, as well as results of fetal karyotyping and FISH evaluation, are reported in Tables 1 and 2. Suspicion of

Table 1 Summary of 15 cases of interrupted aortic arch Type B

Case	*GA (weeks)*	*Referral diagnosis*	*VSD*	*Subclavian artery*	*Aortic arch side*	*Extracardiac anomalies*	*Cytogenetic/FISH aberrations*	*Outcome*
1*	20	Routine	Yes	ARSA	Left	None	22q11 microdeletion	TOP
2*	32	Abnormal heart	Yes	Normal	Left	None	Normal	Alive after surgery
3*	20	Abnormal heart	Yes	ARSA	Left	None	22q11 microdeletion	TOP
4*‡	20	Abnormal heart	Yes	Normal	Left	None	Normal	Dead after surgery
5*	25	Abnormal heart	Yes	Normal	Left	None	22q11 microdeletion	Dead after surgery
6*	26	Abnormal heart	Yes	Normal	Left	None	22q11 microdeletion	Dead after surgery
7*	20	Extracardiac anomalies	Yes	ARSA	Left	Bilateral hydronephrosis	22q11 microdeletion	TOP
8*	32	Persistent extrasystolia	Yes	Normal	Left	None	Normal	Alive after surgery
9†	20	Abnormal heart	Yes	ARSA	Left	None	22q11 microdeletion	TOP
10†	20	Extracardiac anomalies	Yes	Normal	Left	DWM, clubfoot, micrognathia	Trisomy 18	TOP
11†	27	IUGR, polyhydramnios	Yes	ARSA	Left	None	22q11 microdeletion	Died *in utero*
12†	21	Increased NT	Yes	Normal	Left	None	Normal	Alive after surgery
13†	20	Extracardiac anomalies	Yes	Normal	Right	Unilateral kidney agenesis, clubhand	22q11 microdeletion	TOP
14†	29	Mild polyhydramnios	Yes	CORSA	Left	None	22q11 microdeletion	Alive after surgery
15†	32	Mild polyhydramnios	Yes	CORSA	Left	None	22q11 microdeletion	Alive after surgery

*Examined by two-dimensional (2D) echocardiography. †Examined by 2D and 4D echocardiography. ‡Dichorionic twin pregnancy. ARSA, aberrant right subclavian artery; CORSA, cervical origin of right subclavian artery; DWM, Dandy–Walker malformation; FISH, fluorescent *in-situ* hybridization; GA, gestational age; IUGR, intrauterine growth restriction; NT, nuchal translucency; TOP, termination of pregnancy; VSD, ventricular septal defect.

Table 2 Summary of seven cases of interrupted aortic arch Type A

Case	GA (weeks)	Referral diagnosis	VSD	Subclavian artery	Aortic arch side	Extracardiac anomalies	Cytogenetic/FISH aberrations	Outcome
16*	25	Abnormal heart	Yes‡	Normal	Left	None	22q11 microdeletion	Alive after surgery
17*	20	Routine	Yes	Normal	Left	None	Normal	TOP
18*	35	Abnormal heart	Yes	Normal	Left	None	Normal	Alive after surgery
19*	20	Positive family history	No	Normal	Left	None	Normal	Dead after surgery
20†	20	Abnormal heart	No	Normal	Left	Diaphragmatic hernia	Normal	TOP
21†	20	Increased NT	Yes	Normal	Left	None	Normal	Alive after surgery
22†	24	Abnormal heart	Yes	Normal	Left	None	Normal	Alive after surgery

*Examined by two-dimensional (2D) echocardiography. †Examined by 2D and 4D echocardiography. ‡VSD was in subarterial doubly committed position. FISH, fluorescent *in-situ* hybridization; GA, gestational age; NT, nuchal translucency; TOP, termination of pregnancy; VSD, ventricular septal defect.

CHD accounted for nearly half (45%) of the referrals, and two cases were detected during routine ultrasound examination performed by the authors. FISH analysis identified microdeletions in 22q11.2 in 10 of the 15 Type B cases and an unusual association with Type A in one of the seven cases. All cases were *de novo*.

Two-dimensional examination

2D echocardiography allowed us to make the diagnosis of IAA in all 22 cases and the diagnosis of type was correct in 20 of these. In the other two cases (Cases 14 and 21), conventional echocardiography did not allow a conclusive diagnosis of IAA type and a definitive diagnosis was made only after 4D examination.

In six of the seven Type A cases, pronounced asymmetry of the ventricles and great arteries was observed, with the left ventricle being much smaller than the right (Figure 2) and the AAo being much smaller in diameter than the pulmonary artery. In the remaining case (Case 21), there was only slight asymmetry between the left and right ventricles, while asymmetry between the AAo and pulmonary artery was pronounced. In 12 of the 15 Type B cases, there was marked asymmetry only between the AAo and pulmonary artery, with the aorta being much smaller than the pulmonary artery. In the remaining three cases (Cases 2, 4, 14), there was pronounced asymmetry between left and right ventricles. In one of these cases (Case 14), a mild anomaly of the mitral valve was associated.

In IAA Type B, the AAo was observed to run a straight course to the innominate and the left carotid arteries (Figure 3), whereas in Type A there was a slight curvature after the origin of the innominate artery (Figure 4), due to the persistence of the aortic arch segment between the origin of the left carotid and subclavian arteries. In no case was the whole aortic arch visualized in both the sagittal and transverse planes. In the sagittal section, the AAo could be traced into the innominate and the left carotid arteries in IAA Type B (Figure 3), and also into the subclavian artery in IAA Type A (Figure 4), but it could not be traced into the descending aorta.

There was a ventricular septal defect in 20/22 cases (Tables 1 and 2): five of the seven Type A cases and all 15 Type B cases. It was restrictive in three of the five Type A cases (Cases 17, 18, 22) and in two of the 15 Type B cases (Cases 2, 4). Hypo-/aplasia or posterior malalignment of the infundibular septum with narrowing of the left ventricular outflow tract was present in most Type B cases and in one Type A case (Case 16).

In seven of the 15 Type B cases, the right subclavian artery arose anomalously (Table 1). In five of these, 2D echocardiography failed to identify the anomalous origin of the artery: in both cases of cervical origin of the right SA (CORSA) (Cases 14 and 15), which were diagnosed at 4D echocardiography and confirmed postnatally; and in three of the five cases (Cases 1, 3 and 7) of its anomalous origin from the descending aorta, in which, examined only by 2D echocardiography, the aberrant right subclavian artery (ARSA) was revealed by autopsy. Two cases of bicuspid aortic valve (Cases 7 and 8), examined only by 2D echocardiography, were also missed at prenatal diagnosis.

Four-dimensional examination

In the second part of the study, all cases diagnosed with IAA at 2D echocardiography were re-examined by 4D ultrasound with B-flow imaging and STIC (Tables 1 and 2), which enabled clear visualization of the course of the AAo and of the anatomy and route of the neck vessels (Figures 3 and 4).

In all four examined cases of ARSA, 4D ultrasound confirmed or identified its anomalous origin and course. In Cases 9 and 11 it arose from the descending aorta and in Cases 14 and 15 it arose high in the neck from the right common carotid artery (Figure 5). In these latter cases of CORSA, the SA descended down the neck to enter the right arm.

Outcome

There were eight terminations of pregnancy among the 13 fetuses in which IAA was diagnosed before 24 weeks' gestation (Tables 1 and 2). One fetus died *in utero* (Case 11) and four neonates (Cases 4, 5, 6 and 19) died after surgery. One of these (Case 4) had a very low birth weight. The remaining neonates survived surgery.

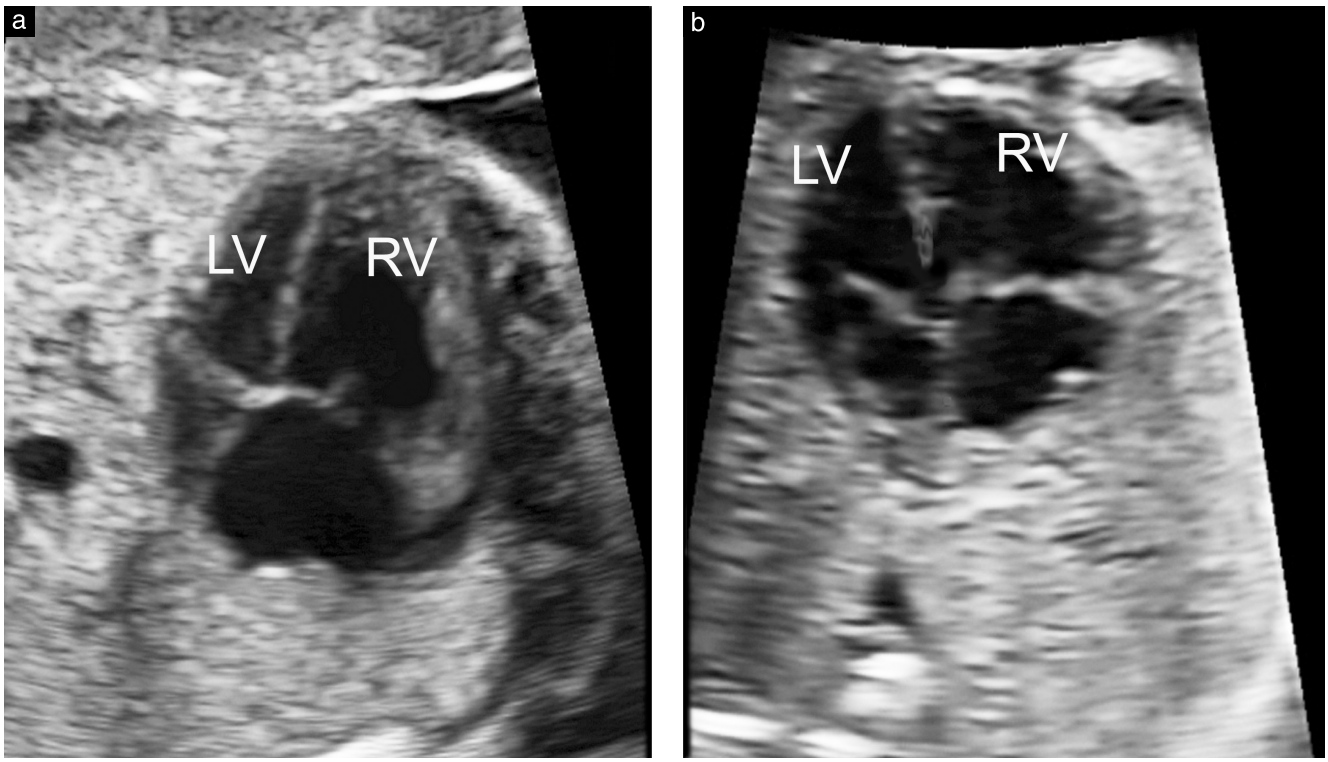

Figure 2 Four-chamber views of the fetal heart at 24 weeks in a case of interrupted aortic arch (IAA) Type A (a) and at 21 weeks in a case of IAA Type B (b). In the Type A fetus there is pronounced asymmetry of the two ventricles, the left (LV) being much smaller than the right (RV), while in the Type B fetus the two ventricles are of approximately equal size and thickness. A ventricular septal defect can be seen.

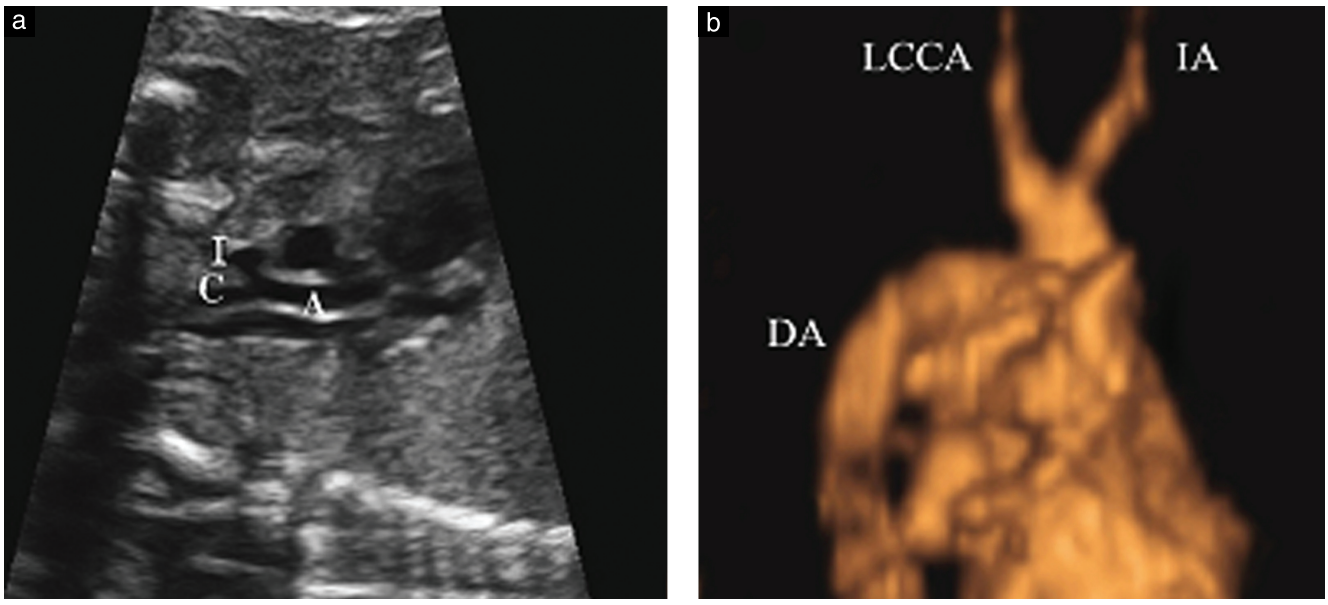

Figure 3 Interrupted aortic arch (IAA) Type B in a 21-week fetus. (a) Two-dimensional echocardiography showing how the ascending aorta (A) fails to curve, but courses straight, cranially, to divide into the innominate artery (I) and the left common carotid artery (C). (b) B-flow and spatiotemporal image correlation showing a typical 'V-shaped' configuration due to the aspect of the ascending aorta, with a straight course to the innominate artery (IA) and the left common carotid artery (LCCA) clearly visible. DA, descending aorta.

One fetus (Case 11) was affected by intrauterine growth restriction (IUGR) at time of diagnosis and another three fetuses successively developed IUGR (Cases 4, 5 and 6). Interestingly, all IUGR fetuses were associated with 22q11.2 microdeletion except Case 4, which was the only twin fetus with IAA in our cases series.

In all neonates with IAA Type B and microdeletion (Cases 5, 6, 14 and 15), characteristic features of DiGeorge syndrome were present: abnormal immunological patterns and decreased parathormone levels, with hypocalcemia requiring calcium supplementation. There was no immunological anomaly in the fetus with IAA

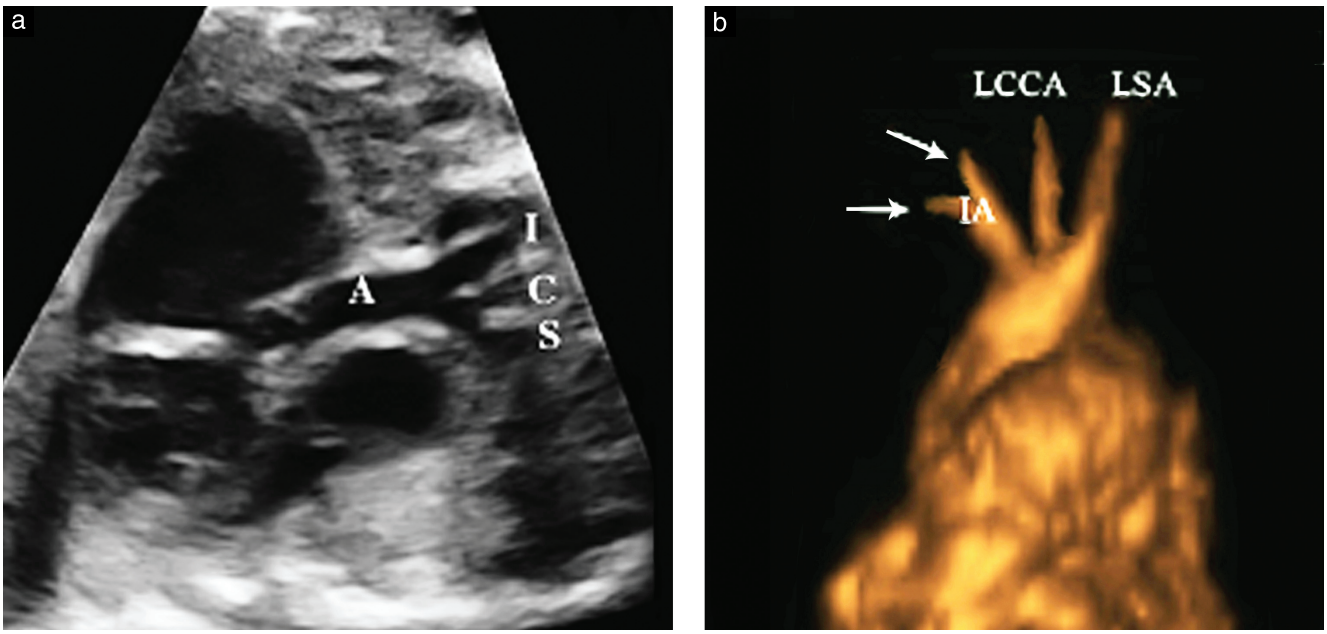

Figure 4 Interrupted aortic arch (IAA) Type A in a 24-week fetus. (a) Two-dimensional echocardiography showing slight curvature of the ascending aorta (A) after the origin of the innominate artery (I), related to the persistence of the aortic arch segment between the origin of the left carotid (C) and subclavian (S) arteries. (b) B-flow and spatiotemporal image correlation clearly showing a typical 'W-shaped' configuration due to the aspect of the innominate artery (IA), the left common carotid artery (LCCA) and the left subclavian artery (LSA). The arrows indicate the right common carotid artery and the right subclavian artery.

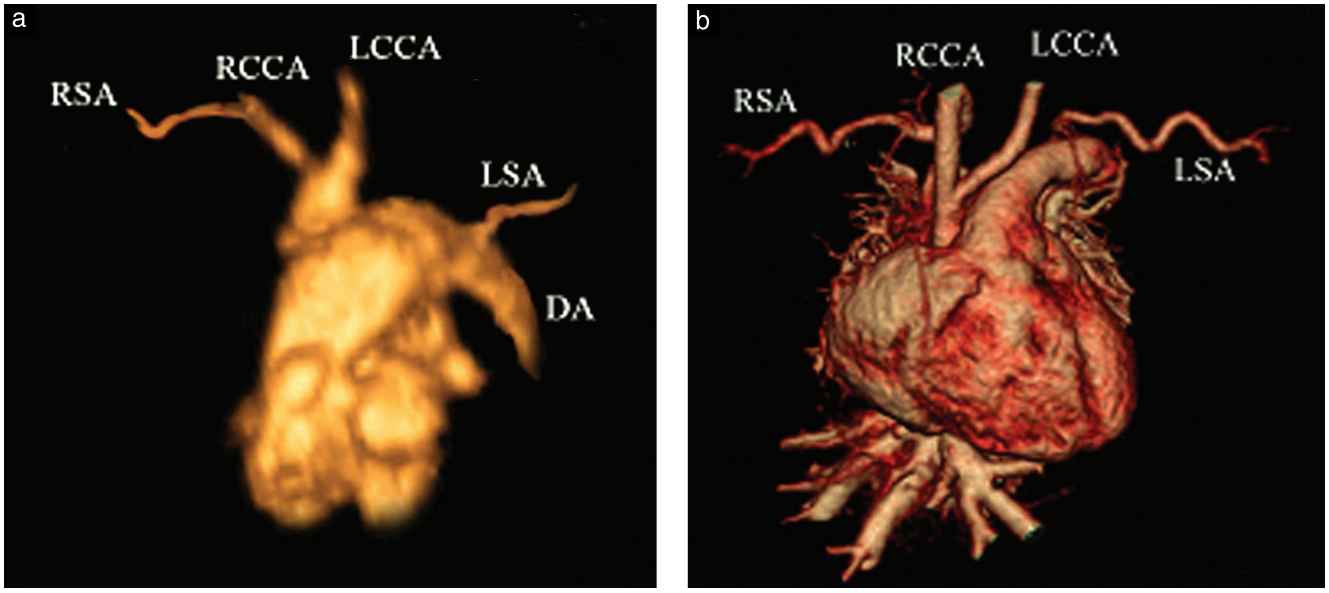

Figure 5 Interrupted aortic arch (IAA) Type B with cervical origin of the right subclavian artery (RSA). The cervical origin from the right common carotid artery (RCCA) is clearly seen both by B-flow and spatiotemporal image correlation prenatally at 29 weeks (a) and by computed tomographic imaging postnatally (b). DA, descending aorta; LCCA, left common carotid artery; LSA, left subclavian artery.

Type A and microdeletion (Case 16): hypocalcemia, T-cell abnormalities, and/or overt thymic hypoplasia were absent.

DISCUSSION

Prenatal diagnosis of IAA and its types has been the subject of very few studies[7,8]. As reported in our case series, the diagnosis of this anomaly depends on the observation of some reliable morphological indicators that point to the correct differential diagnosis.

In the four-chamber view there was an LV/RV size discrepancy in all but one of our cases of IAA Type A, with the LV being much smaller than the RV. This readily detectable sign should be considered as a hint to check the great vessels: angling towards the outflow tracts to image the great vessels revealed a size discrepancy between the great arteries, with the AAo being much smaller in diameter than the main pulmonary artery. In all these cases it is important to check the continuity of the aortic arch. There was no marked discrepancy in ventricular size in most (12/15) IAA Type B cases, whereas

there was a pronounced discrepancy in diameter of the great vessels in all cases. The presence in all these cases of a large VSD probably permitted adequate left ventricular growth. In fact, in the three cases in which there was a marked discrepancy in ventricular size, the left ventricle being much smaller than the right ventricle, there was an associated restrictive VSD (Cases 2 and 4) or mitral valve anomaly (Case 14).

In all our Type B cases the AAo was observed to run a straight course to the innominate and left carotid arteries (the typical V-shape), whereas in Type A cases there was a slight curvature after the origin of the innominate artery, related to the persistence of the aortic arch segment between the origin of the left carotid and subclavian arteries (the typical W-shape). The course of the AAo can be used to distinguish between IAA and coarctation of the aorta; in the former the AAo runs with a straight course to its branches, while in the latter there is normal aortic curvature and continuity with the descending aorta[7,8].

An abnormal origin of the right subclavian artery was observed in seven of the 15 cases of IAA Type B. Fetal examination by 2D echocardiography did not achieve correct diagnosis of these in five cases. The first three cases, in which it arose from the descending aorta, were examined in the 1990s, in the earliest part of the study. The missed diagnoses could reflect inherent limitations of the equipment used in those days, as well as the initial stages of the examiners' increasing experience over time. In the remaining two cases, the latest of our series, the right SA arose high in the neck, which could explain the failure of 2D echocardiography to distinguish the anomalous cervical origin of this small vessel. 4D ultrasound with B-flow imaging and STIC was adopted in the last 10 cases in our series, in each case allowing identification of the anatomical features of IAA and its different types. This technique also permitted clearer identification of the anomalous origin and the course of the right SA, allowing, for the first time, the prenatal diagnosis of CORSA, and confirming that B-flow imaging and STIC are crucial to identifying and tracking the route of thin vessels[15–17]. Cervical origin of the right SA from the right common carotid artery has been reported previously only in postnatal case series; it was described in 1984 by Kutsche and Van Mierop[19], who observed it in four of 21 infants studied for IAA. They saw the origin of the vessel along with the origins of the internal and external carotid arteries as a trifurcation, at the level of the thyroid gland. It then descended down the neck to enter the right arm. The pathogenesis of CORSA can be explained by impairment of fourth aortic arch development, before the involution of the right ductus caroticus (segment of the dorsal aorta between the third and fourth arches)[19].

As confirmed by our study, IAA Type B is usually syndromic, being the most common cardiac defect occurring in DiGeorge syndrome. This is a developmental disease characterized by thymic and parathyroid gland hypo-/aplasia associated with CHD (in $>90\%$ cases) and especially conotruncal malformations[20–22]. CHD is present with a similarly high frequency in patients affected by velocardiofacial syndrome (VCFS), in association with facial dysmorphism, cleft palate and speech and learning disabilities, and in conotruncal anomaly face syndrome (CTFAS), a rare disease with a characteristic facies. These three syndromes are usually associated with microdeletions of segment 22q11.2 (88% of cases in DiGeorge syndrome, 81% in VCFS and 84% in CTFAS)[23–26].

We found the percentage association between IAA Type B and 22q11.2 microdeletion to be high (10/15 cases, 66.7%). Postnatal series confirm the close association between Type B and 22q11.2 microdeletion[4–6], whereas IAA Type A is rarely associated[3]. The remarkably different frequency of association with 22q11.2 deletion suggests that IAA Types A and B could be two separate pathogenetic entities. A possible explanation might lie in the disparate embryological origin of the different segments composing the aortic arch. In fact, hemizygosity for 22q11.2 results in aberrant development of the fourth branchial arch and derivatives of the third and fourth pharingeal pouches[6]. In IAA Type B, the deficient segment of the aorta is the one that normally derives from the left fourth pharyngeal arch, which is inhabited by neural crest cells. In Type A, the atretic or absent segment usually develops from a portion of the left dorsal aorta that is not inhabited by neural crest cells. Alternatively, alterations in cardiac hemodynamics have been suggested to be the pathogenetic mechanism responsible for IAA Type A[27]. At present, we are unable to explain the unusual association of 22q11.2 deletion with IAA Type A detected in one of our cases. It is probable in this rare association that the additional presence of a VSD with the involvement of the infundibular septum played a role, since after migration to the caudal pharyngeal arches, a subpopulation of cardiac crest cells moves into the cardiac outflow tract to participate with other elements in outflow septation of the truncus arteriosus as well as formation of the conotruncal portion of the ventricular septum.

The presence of CORSA has been described as a specific marker for the presence of monosomy 22q11.2[28]. In both of our cases of CORSA, FISH analysis revealed 22q11.2 microdeletion. Of note, all seven cases with anomalous origin of the right SA were associated with IAA Type B. In all these cases 22q11.2 microdeletion was present, while only three of eight cases with normal right SA associated with IAA Type B had this microdeletion, confirming a close association between IAA Type B and microdeletion, if additional aortic arch anomalies are present[5,20,29]. The prenatal finding of 22q11.2 microdeletion enables clinicians to provide the couple with further informative counseling: they should receive information about 22q11.2 microdeletion phenotypic findings, recurrence risk and disease variability, as well as prognosis.

In conclusion, our report confirms the feasibility of the prenatal characterization of IAA and its different types based on 2D echocardiographic examination, albeit with some limitations in the thorough assessment of the pathology, depending on the anatomy of the

defect, the technical adequacy of the equipment used and the experience of the operator. 4D ultrasound with B-flow imaging and STIC is apparently able to facilitate visualization and detailed examination of the anatomical features of IAA and its different types, supplying additional information with respect to 2D fetal sonography. Our data are consistent with previous reports indicating that IAA Types A and B are distinct entities, confirming a close association between IAA Type B and 22q11.2 microdeletion. IAA Type A is not commonly associated with 22q11.2 hemizygosity.

REFERENCES

1. Brierley J, Redington AN. Aortic coarctation and interrupted aortic arch. In *Pediatric Cardiology*, Anderson RH, Macartney FJ, Shinebourne EA, Tynan M (eds). Churchill Livingstone: Edinburgh, UK, 2001; 1523–1551.
2. Hornberger LK. Aortic arch anomalies. In *Textbook of Fetal Cardiology*, Allan L, Hornberger L, Sharland G (eds). Greenwich Medical Media: London, UK, 2000; 305–321.
3. Takahashi K, Kuwahara T, Nagatsu M. Interruption of the aortic arch at the isthmus with DiGeorge syndrome and 22q11.2 deletion. *Cardiol Young* 1999; **9**: 516–518.
4. Lewin MB, Lindsay EA, Jurecic V, Goytia B, Towbin J, Baldini A. A genetic aetiology for interruption of the aortic arch type B. *Am J Cardiol* 1997; **80**: 493–497.
5. Goldmuntz E, Clark BJ, Mitchell LE, Jawad AF, Cuneo BF, Reed L, McDonald-McGinn D, Chien P, Feuer J, Zachai EH, Emanuel BS, Driscoll DA. Frequency of 22q11 deletions in patients with conotruncal defects. *J Am Coll Cardiol* 1998; **32**: 492–498.
6. Rauch A, Hofbeck M, Leipold G, Klinge J, Trautmann U, Kirsch M, Singer H, Pfeiffer RA. Incidence and significance of 22q11.2 hemizygosity in patients with interrupted aortic arch. *Am J Med Genet* 1998; **78**: 322–331.
7. Volpe P, Marasini M, Caruso G, Gentile M. Prenatal diagnosis of interruption of the aortic arch and its association with deletion of chromosome 22q11. *Ultrasound Obstet Gynecol* 2002; **20**: 327–331.
8. Marasini M, Pongiglione G, Lituania M, Cordone M, Porro E, Garello-Cantoni L. Aortic arch interruption: Two-dimensional echocardiographic recognition in utero. *Pediatr Cardiol* 1985; **6**: 147–149.
9. Chaoui R, Hoffmann J, Heling KS. 3D and 4D color Doppler fetal echocardiography using spatio-temporal image correlation (STIC). *Ultrasound Obstet Gynecol* 2004; **23**: 535–545.
10. Goncalves LF, Espinoza J, Lee W, Mazor M, Romero R. Three and four-dimensional reconstruction of the aortic and ductal arches using inversion mode: a new rendering algorithm for visualization of fluid-filled anatomical structures. *Ultrasound Obstet Gynecol* 2004; **24**: 696–698.
11. DeVore GR, Polanko B. Tomographic ultrasound imaging of the fetal heart. A new technique for identifying normal and abnormal cardiac anatomy. *J Ultrasound Med* 2005; **24**: 1685–1696.
12. Espinoza J, Goncalves LF, Lee W, Mazor M, Romero R. A novel method to improve prenatal diagnosis of abnormal systemic venous connections using three- and four-dimensional ultrasonography and 'inversion mode'. *Ultrasound Obstet Gynecol* 2005; **25**: 428–434.
13. Yagel S, Cohen SM, Shapiro I, Valsky DV. 3D and 4D ultrasound in fetal cardiac scanning: a new look at the fetal heart. *Ultrasound Obstet Gynecol* 2007; **29**: 81–95.
14. Paladini D, Volpe P, Sglavo G, Vassallo M, De Robertis V, Marasini M, Russo MG. Transposition of the great arteries in the fetus: assessment of the spatial relationships of the arterial trunks by four-dimensional echocardiography. *Ultrasound Obstet Gynecol* 2008; **31**: 271–276.
15. Volpe P, Campobasso G, De Robertis V, Di Paolo S, Caruso G, Stanziano A, Volpe N, Gentile M. Two- and four-dimensional echocardiography with B-flow imaging and spatiotemporal image correlation in prenatal diagnosis of isolated total anomalous pulmonary venous connection. *Ultrasound Obstet Gynecol* 2007; **30**: 830–837.
16. Pooh RK, Korai A. B-flow and B-flow spatio-temporal image correlation in visualizing fetal cardiac blood flow. *Croat Med J* 2005; **46**: 808–811.
17. Volpe P, Campobasso G, Stanziano A, De Robertis V, Di Paolo S, Caruso G, Volpe N, Gentile M. Novel application of 4D sonography with B-flow imaging and spatio-temporal image correlation (STIC) in the assessment of the anatomy of pulmonary arteries in fetuses with pulmonary atresia and ventricular septal defect. *Ultrasound Obstet Gynecol* 2006; **28**: 40–46.
18. Tan J, Silverman NH, Hoffman JIE, Villegas M, Schmidt KG. Cardiac dimensions determined by cross-sectional echocardiography in the normal human fetus from 18 weeks to term. *Am J Cardiol* 1992; **70**: 1459–1467.
19. Kutsche AM, Van Mierop LHS. Cervical origin of the right subclavian artery in aortic arch interruption: pathogenesis and significance. *Am J Cardiol* 1984; **53**: 892–895.
20. Volpe P, Marasini M, Caruso G, Marzullo A, Buonadonna AL, Arciprete P, Di Paolo S, Volpe G, Gentile M. 22q11 deletions in fetuses with malformations of the outflow tracts or interruption of the aortic arch: impact of additional ultrasound signs. *Prenat Diagn* 2003; **23**: 752–757.
21. Boudjemline Y, Fermont L, Le Bidois J, Lyonnet S, Sidi D, Bonnet D. Prevalence of 22q11 deletion in fetuses with conotruncal cardiac defects: a 6-year prospective study. *J Pediatr* 2001; **138**: 520–524.
22. Chaoui R, Kalache KD, Heling KS, Tennstedt C, Bommer C, Korner H. Absent or hypoplastic thymus on ultrasound: a marker for deletion 22q11.2 in fetal cardiac defects. *Ultrasound Obstet Gynecol* 2002; **20**: 546–552.
23. Van Mierop LHS, Kutsche LM. Cardiovascular anomalies in DiGeorge syndrome and importance of neural crest as a possible pathogenetic factor. *Am J Cardiol* 1986; **58**: 133–137.
24. Fokstuen S, Arbenz U, Artan S, Dutly F, Bauersfeld U, Brecevic L, Fasnacht M, Rothlisberger B, Schinzel A. 22q11.2 deletions in a series of patients with non-selective congenital heart defects: incidence, type of defects and parental origin. *Clin Genet* 1998; **53**: 63–69.
25. Yamagishi H, Grad V, Matsuoka R, Thomas T, Srivastava D. A molecular pathway revealing a genetic basis for human cardiac and craniofacial defects. *Science* 1999; **283**: 1158–1161.
26. Merscher S, Funke B, Epstein JA, Heyer J, Puech A, Lu MM, Xavier RJ, Demay MB, Russell RG, Factor S, Tokooya K, Jore BS, Lopez M, Pandita RK, Lia M, Carrion D, Xu H, Schorle H, Kobler JB, Scambler P, Wynshaw-Boris A, Skoultchi AI, Morrow BE, Kucherlapati R. Tbx1 is responsible for cardiovascular defects in velocardio-facial/DiGeorge syndrome. *Cell* 2001; **104**: 619–629.
27. Clark EB. Mechanisms in the pathogenesis of congenital cardiac malformations. In *Genetics of Cardiovascular Disease*, Pierpont ME, Moller JH (eds). Martinus-Nijhoff: Boston, 1986; 3–11.
28. Rauch R, Rauch A, Koch A, Kumpf M, Dufke A, Singer H, Hofbeck M. Cervical origin of the subclavian artery as a specific marker for monosomy 22q11. *Am J Cardiol* 2002; **89**: 481–484.
29. Rauch R, Rauch A, Koch A, Zink S, Kaulitz R, Girisch M, Singer H, Hofbeck M. Laterality of the aortic arch anomalies of the subclavian artery – reliable indicators for 22q11.2 deletion syndrome? *Eur J Pediatr* 2004; **163**: 642–645.

